Downscaling Atmospheric Teleconnections for the Spring Transition in the Bering Sea

J.E. Overland[1]

N.A. Bond[2]

J.M. Adams[2]

[1]NOAA/Pacific Marine Environmental Laboratory
7600 Sand Point Way NE
Seattle, WA 98115-6349

[2]Joint Institute for the Study of the Atmosphere and Oceans
Box 354235, University of Washington
Seattle, WA 98195-4235

For submission to *Deep-Sea Research II: Topical Studies in Oceanography*

19 October 2000

Contribution No. 2215 from NOAA/Pacific Marine Environmental Laboratory

Abstract

Downscaling relates large-scale (~3000 km) climate variability patterns to regional surface forcing, in this case over the southeast Bering Sea. Climate changes are manifested largely in terms of these large-scale patterns, and it is worthwhile to investigate their contributions, relative to those associated with local variability, in the regional atmospheric forcing. Climate scale patterns in this study are derived from covariance-based EOFs of low-pass filtered (10-day cut-off) 700 mb geopotential height fields for 1958–1999. By design, this EOF analysis elicits sets of patterns for characterizing the variability in the large-scale atmospheric circulation in the Bering Sea. Four modes are considered for each of three periods, January–March, April–May, and June–July. These modes are compared with atmospheric circulation patterns formed by compositing 700 mb height anomalies based on the individual elements constituting the local forcing, i.e., the surface heat and momentum fluxes. In general, different climate modes are associated with different aspects of the forcing. In winter, the modes dominating the forcing of sea ice include considerable interannual variability but no discernible long-term trends. A prominent shift did occur around 1977 in the sign of a winter mode resembling the Pacific-North American (PNA) pattern; the correlation analysis shows this mode to be most significantly related to the local wind stress curl. Decadal variability tends to be more prominent in the leading modes for spring and summer. A pair of modes, one resembling the North Pacific (NP) pattern and one reflecting the strength of the Aleutian low, exhibit long-term trends with implications for the wind forcing during spring. In summer, an NP-like mode and a mode featuring a center over the Bering Sea include long-term trends with impacts on surface heating and wind mixing, respectively.

1. Introduction

The oceanic ecosystem of the Bering Sea has variability on timescales from intraseasonal to interdecadal. Much of this variability is attributable to physical properties of the system, and in particular, to the atmosphere as a fundamental source. It is not yet clear, however, exactly which aspects of the atmospheric forcing are crucial to the Bering Sea ecosystem.

It does appear that the atmospheric variability on decadal timescales is important. Recent research on long-lived (multi-year) species in the Bering Sea indicates that their populations vary more on decadal than on interannual timescales (Beamish et al., 1999). These longer-term variations tend to be synchronous with fluctuations in some of the large-scale modes of climate variability for the North Pacific (Hare and Mantua, 2000). But understanding of the causes of these relationships is limited, because the linkages between climate and ecosystems are complex. Here we address one element of the linkage: the relationship between the large-scale modes of climate variability and the local air-sea interactions that constitute the actual atmospheric forcing.

We make use of the concept of downscaling (Gyalistras et al., 1994). Downscaling has generally referred to relating output from General Circulation Models (GCMs), with resolutions of hundreds of kilometers, to specific conditions at certain locations, such as surface temperatures or rainfall. This approach is used because GCMs generally lack the spatial resolution or physics to characterize local processes. Such relations can be established with high-resolution regional models, statistical techniques, or physical parameterizations. Here we relate large-scale modes of atmospheric variability, also called teleconnections, to parameters important to local forcing of the eastern Bering Sea (Bond and Adams, this issue). Downscaling is meaningful in our application because it is through these large-scale teleconnection modes that potential climate change will be manifest most clearly (Palmer, 1999). We wish to examine how well these modes can specify the variability in local forcing of the Bering Sea.

We construct sets of teleconnection modes using empirical orthogonal function (EOF)/Principal Component (PC) analysis applied to atmospheric circulation data as represented

by geopotential height at 700 mb. EOFs are spatial patterns that represent a reduced basis set for characterizing the variability. The PCs are the time-dependent coefficient weights of the individual EOF patterns. Essentially, the EOF analysis filters out the small-scale, intermittent variability from the more robust aspect, the large-scale, low-frequency variability (LFV).

Many analyses of climate variability for the North Pacific concentrate on winter months (Overland et al., 1999), yet much of the variability important to the Bering Sea ecosystem occurs in the spring and early summer. Previous analyses of teleconnection patterns (Barnston and Livesey, 1987) indicate major changes in the nature of North Pacific teleconnection patterns between winter and spring. Thus our analyses cover the transition between winter and summer, i.e., January through July.

Three different elements of the air-sea interaction in the Bering Sea are considered: the surface heating, the wind forcing of the ocean circulation, and the wind-induced mixing (Bond and Adams, this issue). The importance of the individual forcing mechanisms varies seasonally, and so we examine different sets of these parameters during different seasons. Time series for these parameters and for the 700 mb geopotential heights used in other aspects of the analysis were extracted from the National Center for Environmental Prediction (NCEP)/National Center for Atmospheric Research (NCAR) Reanalysis data set (Kalnay et al. 1996) for the period 1958–1999. For each local parameter and each period, we determined the atmospheric circulation anomalies that correspond with its fluctuations. This was accomplished by forming spatial composites of the 700 mb height for the 1/3 highest and 1/3 lowest values of the local parameter, and differencing them. These difference patterns were then spatially correlated with the 700 mb teleconnection modes from the EOF analysis. This procedure shows the degree to which variations in the regional atmospheric forcing can be attributed to the leading modes of the climate variability. The results include not just measures of the explained variance, but also information on the types of circulation anomalies that are related to each element of the forcing.

2. Modes of North Pacific Variability

2.1. Previous Results

Here we present a brief survey of previous teleconnection studies with relevance to the North Pacific and Bering Sea. This survey is more a sampler than a comprehensive review; its goal is to set the stage for our own results.

Classical weather typing seeks to reduce the spatial variability represented by individual realizations of the atmospheric circulation to a highly limited, but physically relevant, set of patterns. Early approaches were subjective; later approaches have generally been based on semi-objective techniques such as EOF and cluster analysis, and probability density functions (PDFs). An early subjective study identified 22 separate weather patterns for Alaska (Putnins, 1966). Overland and Hiester (1980) used both subjective and automated techniques to establish six patterns for the Gulf of Alaska. Recently 13 major atmospheric circulation patterns for January and July were established by subjective analyses by Mock et al. (1998) for Beringia (the Bering Sea plus portions of the adjacent continents). Mock noted patterns that were both centered on the Bering Sea and those that had east-west gradients in properties across the region.

Objective analyses of 700 mb or 500 mb geopotential height data tend to be more conservative in the number of patterns selected for the North Pacific. Cluster analysis (Cheng and Wallace, 1993; Smyth et al., 1999) and studies based on PDFs (Kimoto and Ghil, 1993a, b; Corti et al., 1999) indicate two fundamental states for the circulation over the North Pacific during winter. These two states reflect the positive and negative phases of the Pacific North American (PNA) teleconnection mode. In essence, the PNA acts to either enhance (in its positive state) or suppress (in its negative state) the climatological pressure differences between the Aleutian low and a ridge over the Canadian Rocky mountains. The variations in the PNA are characterized by a bimodal rather than Gaussian distribution, i.e., significantly positive and negative anomalies are preferred states. Renwick and Wallace (1996) found that the PNA projects substantially onto persistent, high-amplitude troughs and ridges that are favored near the longitude of the climatological Aleutian low (Dole and Gordon, 1983). These features are

somewhat distinct from the canonical PNA anomalies in that they tend to be limited in their east-west extent.

Two additional robust modes have been identified for the North Pacific in winter. The West Pacific (WP) mode, which consists of a north-south dipole over the far western Pacific, relates to the strength and latitude of the tropospheric jet and its associated storm track extending off of Asia and across the western and central Pacific (e.g., Barnston and Livezey 1987; Wallace et al., 1992). The Arctic Oscillation (AO) (Thompson and Wallace, 1998) is an annular mode involving pressure anomalies of opposite signs in the Arctic and at mid-latitudes, with consequences for the nature and latitude of the polar vortex. Among its other impacts, the AO modulates the strength of the Aleutian low (Overland et al., 1999).

Relatively little analysis has been carried out on the modes for spring and summer. The study of Barnston and Livezey (1987) using rotated EOFs included specification of the leading teleconnection modes throughout the year, but little discussion of the modes found for spring and summer. It is noteworthy that the leading mode in spring for the area of interest, the North Pacific (NP) mode, consists of a north-south dipole rather than the east-west wave-like pattern of the PNA. The leading modes found by Barnston and Livezey (1987) for the summer included relatively weak amplitudes over the North Pacific and Bering Sea, but Wallace *et al.* (1993) noted an AO-like hemispheric seesaw between polar and temperate latitudes in summer with relevance to conditions in the Bering Sea.

2.2. Results of Regional EOF Analysis

The objective of our EOF analysis is to isolate the modes responsible for atmospheric variability in the Bering Sea. Because of this regional focus, we use a restricted domain, but one large enough such that the calculated modes are physically meaningful and not strongly impacted by boundary effects. As a reasonable compromise, our domain extends from 20°N to 80°N, and 90°E to 90°W, with the data on a 2.5° by 2.5° grid. Two other aspects of our analysis were designed to bring out the variability in the Bering Sea. First, we based the EOF analysis on

covariances in the 700 mb height, rather than correlations, effectively giving preference to the greater amplitude variations in the northern portion of the domain. Also, we chose not to follow the procedure often used in previous studies in which a cosine of latitude weighting is applied to correct for equal area. Our experiments in this regard indicated that such a procedure emphasized the effects of variability in the southern portion of the domain, and accentuated boundary effects in the northern portion.

Our treatment of the time domain retains the sub-monthly variability but removes the high-frequency variability. This is accomplished by low-pass filtering the data with a 10-day cut-off while sampling every 5 days. This procedure is consistent with the results of Bond and Adams (this issue), which indicates the forcing of the Bering Sea, and its response in terms of SST, are more closely linked to changes in weather regimes of roughly 1–2 week duration than individual weather disturbances on timescales of 1–3 days.

We use EOFs as they capture the most variance by construction. Their shortcoming is that the second and higher patterns are constrained to be mathematically orthogonal to the lower-order patterns; this is not a requirement of the natural system. Different statistical techniques, e.g., rotated EOF analysis, yield somewhat different, but often similar, patterns of variability. The modes used here can be considered typical of those presented and discussed in previous studies concerning the climate variability of the North Pacific. We expect that details in the teleconnection modes, in particular the procedure used to calculate them, are secondary to the primary relationships between these modes and the parameters representing the local forcing of the Bering Sea.

The covariance-based EOF analysis was first carried out on within-monthly samples over the 42 years. Inspection of the EOF patterns for individual months suggested grouping months by January-February-March, April-May, July-July. The analyses were redone for these periods; the resulting EOF patterns are shown in Fig. 1–3. The explained variance of the first 15 modes for the three periods are shown in Fig. 4. In each period, the first three EOFs are distinct by the criteria of North et al. (1982). The principal component time series are shown in Fig. 5.

The EOF modes for January–March (Fig. 1) are described here in terms of their spatial patterns, and how they compare with the modes identified in the previous studies. The leading mode (PC1) features a prominent pole in western Alaska and a broad region of opposite sign across the subtropical Pacific. This mode accounts for almost 20% of the variance and represents primarily the strength of the flow across the central Pacific, with some projection onto the intensity of the Aleutian low. The second mode (PC2) is a dipole with centers of action in northeastern Siberia and the central Pacific and bears some resemblance to the leading North Pacific mode identified by Wallace et al. (1992). This mode is related to variability in the jet stream off of Asia and across the Pacific, and hence north/south displacements of the storms from their typical tracks, and the propensity for lower-tropospheric anti-cyclones, and their associated arctic air masses, to build-up over Siberia. We refer to this mode as the Siberian pattern, as it relates to an index formed by the difference in pressure between the Siberian high and the Aleutian low favored by Russian authors (Tarasenko and Yagudin, 1982). The Siberian mode includes some projection onto the AO as defined by Thomson and Wallace (1998). The third mode (PC3) is a close analog to the PNA, with its prominent poles south of the Aleutians, and over (and north) of western North America. The amount of explained variance drops off considerably for the fourth mode (PC4), which features a wave-like pattern with centers in central Siberia, the Bering Sea, and off western North America.

The EOF modes for April–May (Fig. 2) are distinct from their January–March counterparts. Their patterns are different, their amplitudes are weaker, and their explained variances are smaller. The first mode (PC1) consists of a north/south pressure seesaw between 70°N and 40°N centered at the dateline. This mode is similar to the NP mode found by Barnston and Livezey (1987) and relates to the storminess across the Bering Sea. The second mode (PC2) consists largely of a single center of action over the Aleutians, and relates to the strength of the Aleutian low, which remains an important weather phenomenon into spring. An east-west dipole with a broad center in Siberia and a better-defined pole in the Gulf of Alaska was found for the third mode (PC3). This mode will also be referred to as the Siberian pattern. The fourth mode

(PC4) consists of a wave-like pattern including centers of action in the western Bering Sea and in the northeast Pacific.

The EOF modes for June–July (Fig. 3) continue the trend towards weaker amplitudes and smaller explained variances with the seasonal warming. Not surprisingly, there is also a seasonal trend for the variability to be emphasized in the northern portion of the domain. The first mode (PC1) includes centers of action north of both Siberia and western North America. The second mode (PC2) includes a single prominent center of action north of Bering Strait extending out over the Gulf of Alaska. This mode resembles the NP-like PC1 of April–May, with perhaps the additional influence of the AO. It is related to the frequency and intensity of storms across the Bering Sea. These storms are weaker than their counterparts during winter, but still strongly influence air-sea interactions during summer. The third and fourth modes consist of a single main center near 50°N, 160°W (PC3) and a wave-like pattern with centers in central Siberia, the Bering Sea, and south of the Gulf of Alaska (PC4).

3. Connections between teleconnection modes and regional forcing

Composite 700 mb geopotential height fields were constructed to determine the circulation anomalies associated with major variations in the local air-sea interaction, i.e., atmospheric forcing, parameters. Table 1 lists the parameters considered and the locations where they were evaluated; these selections follow the results of Bond and Adams (this issue). The composite height fields were formed by selecting the periods of 1/3 highest value, and of 1/3 lowest value, for each parameter of interest. The height fields for each set were then differenced to yield a single map that characterizes the changes in the circulation that cause changes in the individual parameters comprising the forcing. These maps were then spatially correlated with the leading four EOF patterns for all three periods; the results are itemized in Tables 2–4. The magnitudes of these correlations quantify the degree to which an individual element of the forcing is related to a particular teleconnection mode.

The nature of the composite maps generated by the procedure outlined above is

illustrated with a sample set of maps pertaining to the net surface heating (Fig. 6). This set of maps shows that the circulation anomalies associated with a particular type of forcing anomaly can change seasonally. In the winter, anomalous heating (cooling) tends to occur during periods of anomalous southerly (northerly) flow in association with suppressed (enhanced) surface fluxes of sensible and latent heat. A virtually identical sense to the flow is associated with anomalous heating during spring. The magnitudes of the fluctuations in the 700 mb height anomalies are generally weaker in spring than in winter. This trend continues into summer, but in this case the character of the circulation anomalies is markedly different. Enhanced heating in summer tends to occur in conditions of high pressure and anomalous northeasterly flow off Alaska. This type of flow tends to be more continental than maritime, and subsequently includes fewer low clouds, and hence, increased downward shortwave (solar) heat fluxes, which represent the dominant source of variability in the surface heating in summer.

The two most important aspects of the regional forcing during winter are those related to sea-ice, and to wind forcing of the ocean circulation. Regarding sea ice, the two fundamental elements of the forcing, the cross-shelf momentum flux or wind stress and the net surface heating (e.g., Overland and Pease, 1982), are most strongly correlated with modes PC2 (Siberian) and PC1, respectively. The net surface flux also has a weaker relation with modes PC2 and PC3 (Siberian and PNA). Three different, but related elements of the wind forcing are expected to be of potential importance in winter. The curl of the surface stress, which is important to the circulation of the deep Bering basin on timescales of a season and longer, is related to PC4 with also a significant contribution by PC3. The along-shelf and along-peninsula momentum fluxes, which would tend to be of more local importance and operating on timescales of less than a year, are most strongly related to modes PC1 and PC2, respectively. It is interesting to note that the PNA-like mode PC3 is not the leading mode for any of the individual forcing parameters.

Springtime in the Bering Sea brings spells of weather both typical of winter and of summer. The wind forcing of the ocean circulation remains significant while the surface heating

begins to set up the warm season stratification. Considering the wind-forcing, the wind stress curl is linked largely to PC2 (the mode related to the strength of the Aleutian low), while the along-shelf and especially the along-peninsula momentum fluxes are most strongly related to PC1 (the NP mode). Mixing is related to the NP mode. With respect to the heating, both the downward shortwave and net heat fluxes are best, but oppositely, correlated with PC3 (Siberian); there is a secondary impact from PC1 (NP). Favorable ice melt conditions would relate to PC3 in both cross shelf momentum and net surface flux.

During summer, the key aspects of the forcing involve the wind mixing, and the surface heating. The wind forcing of the circulation tends to be relatively weak, but is still potentially significant in locations (such as over the shelf and along its shelf-break with the deep Bering Sea basin) where the mean flow is modest and the variability is significant (Stabeno et al., 1999). The wind mixing is correlated best with PC4, and to a lesser extent, with PC3, which have pressure gradients centered over the Bering. The PC4 mode relates to the pressure over the central Bering and hence the propensity for the rare strong cyclonic disturbance during the warm season. The downward shortwave fluxes are also most strongly related to PC4, and to a lesser extent, with PC3, while the net heat fluxes are correlated almost equally with PC2 and PC3. It is worth noting the opposite signs for the correlations between the net heat and downward shortwave and PC3. Apparently, easterly flow anomalies bring about increased solar heat fluxes but these fluxes are more than compensated by other sources of anomalous cooling, namely a combination of increased surface latent heat fluxes (evaporative cooling) and reduced downward longwave fluxes in association with a relatively dry continental air mass.

4. Time series of teleconnection modes

The time series of the winter teleconnection modes (Fig. 5) found in this study exhibit largely interannual rather than decadal scale variability. This is particularly true for modes PC1 and PC2 before 1989, the two modes best correlated with the mechanisms responsible for sea ice on the Bering Sea shelf. Since our analysis was designed to bring out the variability

characterizing the Bering Sea and its forcing, our results are consistent with Bond and Adams (this issue), which found considerable year-to-year fluctuations in wintertime conditions and forcing but little in the way of long-term trends. An exception to this tendency for largely interannual variability is indicated by our time series for PC3, which represents a proxy for the leading mode of the North Pacific as a whole, the PNA. The time series shown in Fig. 5 for PC3 does reveal the step-like change in 1977 associated with the well-publicized "regime shift" for the North Pacific. But its implications for the Bering Sea are limited for two reasons. This mode is only the third-most important in accounting for the wintertime variability in our analysis, and it is also only modestly correlated with the local forcing parameters in the Bering Sea. It does have a significant projection onto the pattern of circulation anomalies associated with the wind stress curl which itself tends to be more important on long (multi-year) timescales. Another exception to this tendency for mostly interannual variability is represented by the shift in our Siberian mode (PC2) in the late 1980s. This change is coincident with a major swing in the sense of the wintertime AO.

The time series of our teleconnection modes for spring and summer (Fig. 5) exhibit some important differences from their winter counterparts. In particular, PC1 and PC2 in April–May and PC2 and PC4 in June–July, include substantial decadal variability or long-term trends. The modes representing the NP in spring (PC1) and summer (PC2) were of the sense to contribute towards anomalously high pressures over the Bering Sea and Alaska during most of the 1990s. A reversal in PC1 occurred for the spring in 1998, but not for PC2 for the summer. Our time series for these modes mimics the time series of the NP mode calculated (and maintained) by NCEP (not shown) using the procedure of Barnston and Livezey (1987). As shown by the correlations in Table 3 and 4, these persistent anomalies in the NP have had implications principally on the wind-forcing in spring and the net surface heat fluxes in summer. The systematic trend towards warmer summertime conditions over the Bering Sea shelf found by Bond and Adams (this issue) can be attributed in large part to the trends in the leading teleconnection modes characterizing the atmospheric circulation during spring and summer.

5. Summary

This study has investigated how large-scale atmospheric teleconnection patterns relate to local air-sea interaction parameters for the Bering Sea. Climate changes, either due to natural variability or anthropogenic influences, are manifested through these teleconnection patterns, and our results show the degree to which these changes are accompanied by changes in the actual forcing of the ocean by the atmosphere. The teleconnection modes we use are based on an EOF analysis of 700 mb heights for the period 1958–1999. The analysis is designed to yield the modes that best capture the low-frequency variability (greater than 10 days) of the Bering Sea. The four leading modes for three periods, January–March, April–May, and June–July, are compared with the modes identified in previous studies, and with composite circulation anomalies associated with individual components of the atmospheric surface forcing. Different teleconnection modes map on different components of the forcing, and the most prominent sources of atmospheric variability do not necessarily play the most important roles in crucial aspects of the forcing.

In winter, the first and second leading modes are best correlated with the two aspects of the forcing crucial to sea ice over the shelf, the net surface heat flux and cross-shelf momentum flux. The third mode, which resembles the well-known PNA pattern, is related to the wind stress curl, but otherwise projects only modestly upon the individual parameters making up the wintertime forcing. The leading mode in spring resembles the previously identified NP mode, and is strongly related to various aspects of the wind forcing. The second and third modes project significantly onto the composites characterizing anomalies in the wind stress curl and the surface heat fluxes, respectively. In summer, the leading four modes explain significantly less variance than their winter and spring counterparts. Of particular importance is the second mode, with a resemblance to the NP and an impact on the net surface heat fluxes. The third and fourth modes are most strongly related to the other crucial aspect of the summertime forcing, i.e., the wind mixing.

A particularly interesting result is the differences in the character of the time series of the

leading modes for the Bering Sea in winter, relative to spring and summer. The winter modes feature considerable interannual variations and sharp transitions, but little in the way of systematic long-term trends. There is a substantial shift in PC3, the PNA-like mode, in association with the North Pacific's regime shift of 1976/77. A less prominent, but notable, change occurred in PC2, the Siberian mode, in the late 1980's during a major reversal of the AO. But for the most part, many of the leading modes for spring and summer include much more in the way of substantial decadal variability or even systematic long-term trends. The NP-like modes in particular exhibit this behavior, with important implications for both wind forcing and increases in surface heating. The north/south dipole configuration of the NP presumably makes it sensitive to physical processes involving both the North Pacific and the Arctic. The changes in the spring/summer Arctic climate that are presently occurring therefore could potentially have important remote effects on the Bering Sea.

Acknowledgments

We appreciate the support from the North Pacific Marine Research (NPMR) Initiative. This publication is FOCI contribution # B401 and PMEL contribution # 2215, and was supported by the Joint Institute for the Study of the Atmosphere and Ocean (JISAO) under NOAA Cooperative Agreement #NA67RJO155, Contribution #801.

References

Barnston, A.G., Livezey, R.E., 1987. Classification, seasonality and persistence of low frequency atmospheric circulation patterns. Monthly Weather Review 115, 1083–1126.

Beamish, R.J., Noakes, D.J., McFarline, G.A., Klyashtorin, L., Ivanov, V.V., Kurashov, V., 1999. The regime concept and natural trends in the production of Pacific salmon. Canadian Journal of Fisheries and Aquatic Sciences 56, 516–526.

Bond, N.A., Adams, J.M., 2000. Atmospheric forcing of the southeast Bering Sea Shelf during 1995–99 in the context of a 40-year historical record. Deep-Sea Research II: Topical Studies in Oceanography (submitted).

Cheng, X., Wallace, J.M., 1993. Cluster analysis of the northern hemisphere wintertime 500-hPa height field: Spatial patterns. Journal of the Atmospheric Sciences 50, 2674–2696.

Corti, S., Molteni, F., Palmer, T.N., 1999. Signature of recent climate change in frequencies of natural atmospheric regimes. Nature 398, 799–802.

Dole, R.M., Gordon, N.D., 1983. Persistent anomalies of the extratropical Northern Hemisphere circulation: Geographical distribution and regional persistence characteristics. Monthly Weather Review 111, 1567–1586.

Gyalistras, D., von Storch, H., Fischlin, A., Beniston, M., 1994. Linking GCM-simulated climate changes to ecosystem models: Case studies of statistical downscaling in the Alps. Climate Research 4, 167–189.

Hare S.R., Mantua, N.J., 2000. Empirical evidence for North Pacific regime shifts in 1977 and 1989. Progress in Oceanography, in press.

Kalnay, E., and co-authors, 1996. The NCEP/NCAR 40-year reanalysis project. Bulletin of the American Meteorology Society 77, 437–471.

Kimoto, M., Ghil, M., 1993a. Multiple flow regimes in northern hemisphere winter. Part I: Methodology and hemisphere regimes. Journal of the Atmospheric Sciences 50, 2625–2643.

Kimoto, M., Ghil, M., 1993b. Multiple flow regimes in the northern hemisphere winter. Part II:

Sectorial regimes and preferred transitions. Journal of the Atmospheric Sciences 50, 2645–2673.

Mock, C.J., Bartlein, P.J., Anderson, P.A., 1998. Atmospheric circulation patterns and spatial climatic variations in Beringia. International Journal of Climatology 10, 1085–1104.

North, G.R., Bell, T.L., Cahalan, R.F., Moeng, F.J., 1982. Sampling errors in the estimation of EOFs. Monthly Weather Review 110, 699–706.

Overland, J.E., Hiester, T.R., 1980. Development of a synoptic climatology for the northeast Gulf of Alaska. Journal of Applied Meteorology 19, 1–14.

Overland, J.E., Pease, C.H., 1982. Cyclone climatology of the Bering Sea and its relation to sea ice extent. Monthly Weather Review 110, 5–13.

Overland, J.E., Adams, J.M., Bond, N.A., 1999. Decadal variability of the Aleutian low and its relation to high latitude circulation. Journal of Climate 12, 1542–1551.

Palmer, T.N., 1999. A non-linear dynamical perspective on climate prediction. Journal of Climate 12, 575–591.

Putnins, P., 1966. The sequence of baric pressure patterns over Alaska. Studies of the Meteorology of Alaska, First Interim Report, Environmental Data Service, ESSA, Washington, D.C., 57 pp.

Renwick, J.A., Wallace, J.M., 1996. Relationships between the North Pacific wintertime blocking, El Niño, and the PNA pattern. Monthly Weather Review 124, 2071–2076.

Smyth, P., Ide, K., Ghil, M., 1999. Multiple regimes in northern hemisphere height fields via mixture model clustering. Journal of the Atmospheric Sciences 56, 3704–3723.

Stabeno, P.J., Schumacher, J.D., Ohtani, K., 1999. The physical oceanography of the Bering Sea. In: Loughlin, T.R., Ohtani, K. (Eds.), Dynamics of the Bering Sea, North Pacific Marine Science Organization (PICES), University of Alaska Sea Grant.

Tarasenko, V.D., Yagudin, R.A., 1982. About the influence of the Pacific AAC on the formation of air temperature anomaly of West Siberia. In: Proceedings of Western Siberian Regional Hydrometeorological Research Institute 54, 20–27.

Thompson, D.W.J., Wallace, J.M., 1998. The Arctic oscillation signature in the wintertime geopotential height and temperature fields. Geophysical Research Letters 25, 1297–1300.

Wallace, J.M., Smith, C., Bretherton, C.S., 1992. Singular value decomposition of wintertime sea surface temperature and 500-mb height anomalies. Journal of Climate 5, 561–576.

Wallace, J.M., Zhang, Y., Lau, K., 1993. Structure and seasonality of interannual and interdecadal variability of the geopotential height and temperature fields in the northern hemisphere troposphere. Journal of Climate 6, 2063–2082.

TABLE 1

Local variable locations (Latitude, longitude)

Cross-shelf momentum flux	57.2, 164.1
Along-shelf momentum flux	55.3, 169.7
Along-peninsula momentum flux	53.4, 173.4
Net surface flux (during winter)	55.3, 171.6
Net surface flux (during spring and summer)	57.2, 164.1
Downward shortwave flux	57.2, 164.1
Mixing	57.2, 164.1
Wind stress curl	55.3, 175.1

TABLE 2

Correlation results for January–March

Name	PC1	PC2 Siberian	PC3 PNA	PC4
Cross-shelf momentum flux	–0.27	–0.77	0.23	–0.45
Along-shelf momentum flux	–0.80	–0.03	0.34	–0.26
Along-peninsula momentum flux	0.21	–0.88	–0.01	–0.15
Wind stress curl	0.37	0.17	0.53	0.63
Net surface flux	–0.77	–0.40	0.32	–0.10

TABLE 3

Correlation results for April–May

Name	PC1	PC2	PC3	PC4
	NP		Siberian	
Cross-shelf momentum flux	0.47	0.07	0.66	0.66
Along-shelf momentum flux	–0.64	–0.31	0.52	0.28
Along-peninsula momentum flux	0.88	0.12	0.22	0.40
Mixing	0.77	0.50	0.04	0.25
Wind stress curl	0.32	0.73	0.23	0.40
Net surface flux	–0.40	0.16	0.72	0.39
Downward shortwave flux	–0.36	0.03	–0.70	–0.57

TABLE 4

Correlation results for June–July

Name	PC1	PC2 NP	PC3	PC4
Along-shelf momentum flux	0.44	–0.59	0.16	–0.42
Along-peninsula momentum flux	0.03	0.57	–0.52	–0.28
Mixing	0.27	0.26	–0.41	–0.57
Net surface flux	–0.16	–0.50	–0.48	0.32
Downward shortwave flux	–0.14	–0.13	0.50	0.63

Figure Captions

Fig. 1. Patterns of 700 mb geopotential height anomalies of the four leading EOF modes for January through March. Solid (dashed) contours refer to positive (negative) heights with an interval of 5 m and the zero contour is omitted. The numbers in the upper right-hand portion of each panel refer to the percentage of variance explained by each mode.

Fig. 2. As in Fig. 1, but for April–May.

Fig. 3. As in Fig. 1, but for June–July.

Fig. 4. Percentage of variance explained by each of the fifteen leading EOF modes for January–January–March (top), April–May (middle), and June–July (bottom). The total percentage of the variance explained by these 15 modes is noted in each panel.

Fig. 5. Time series of the principal components of the four leading EOF modes for January–March (left column), April–May (middle column), and June–July (right column). Each value represents an average for the particular year.

Fig. 6. Composite 700 mb height anomaly maps pertaining to anomalies in the net surface heat flux in January–March (top; contour interval 20 m), April–May (middle; contour interval 20 m), and June–July (bottom, contour interval 10 m). See text for details.

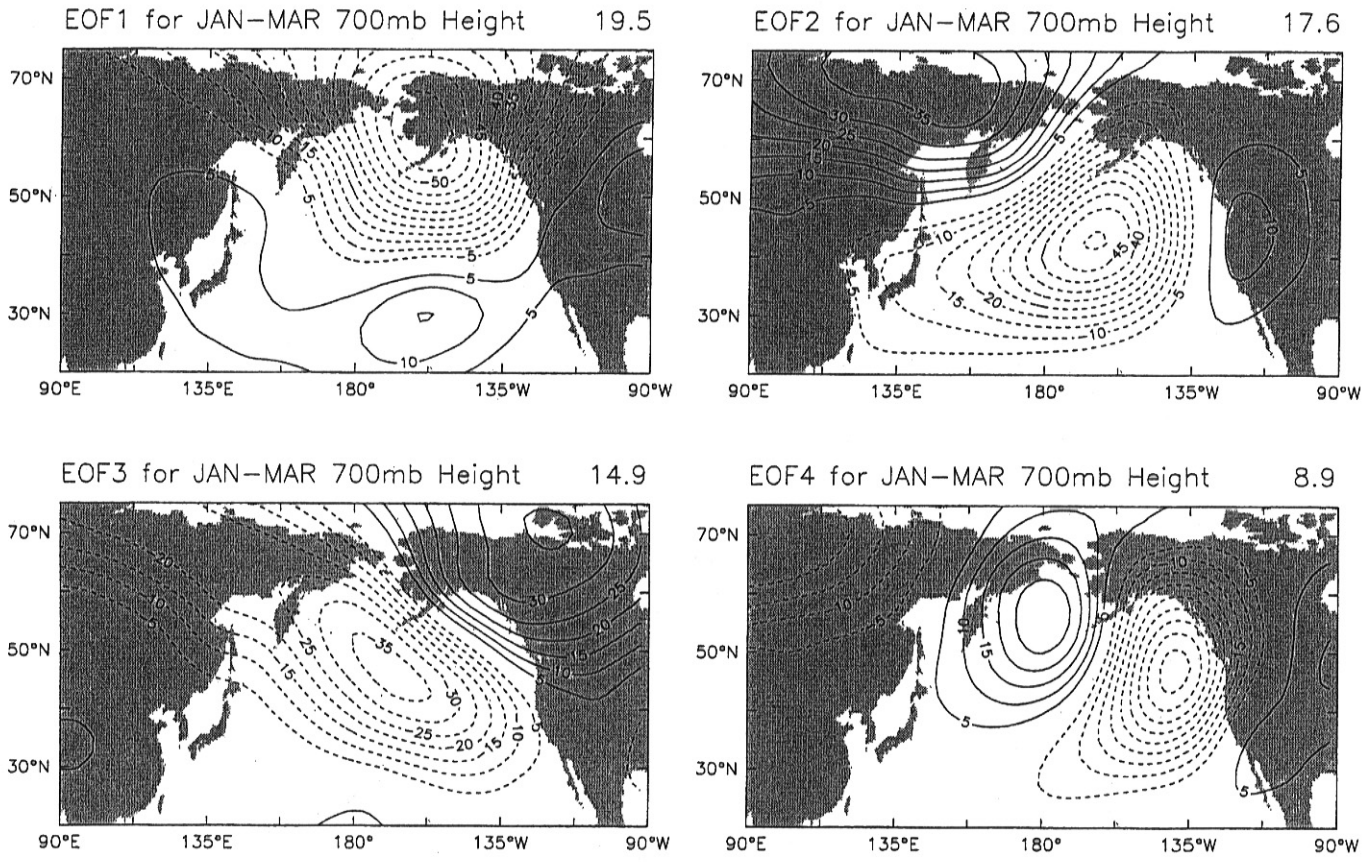
EOF1 for JAN–MAR 700mb Height 19.5
EOF2 for JAN–MAR 700mb Height 17.6
EOF3 for JAN–MAR 700mb Height 14.9
EOF4 for JAN–MAR 700mb Height 8.9
70°N
50°N
30°N
90°E
135°E
180°
135°W
90°W

Fig. 1

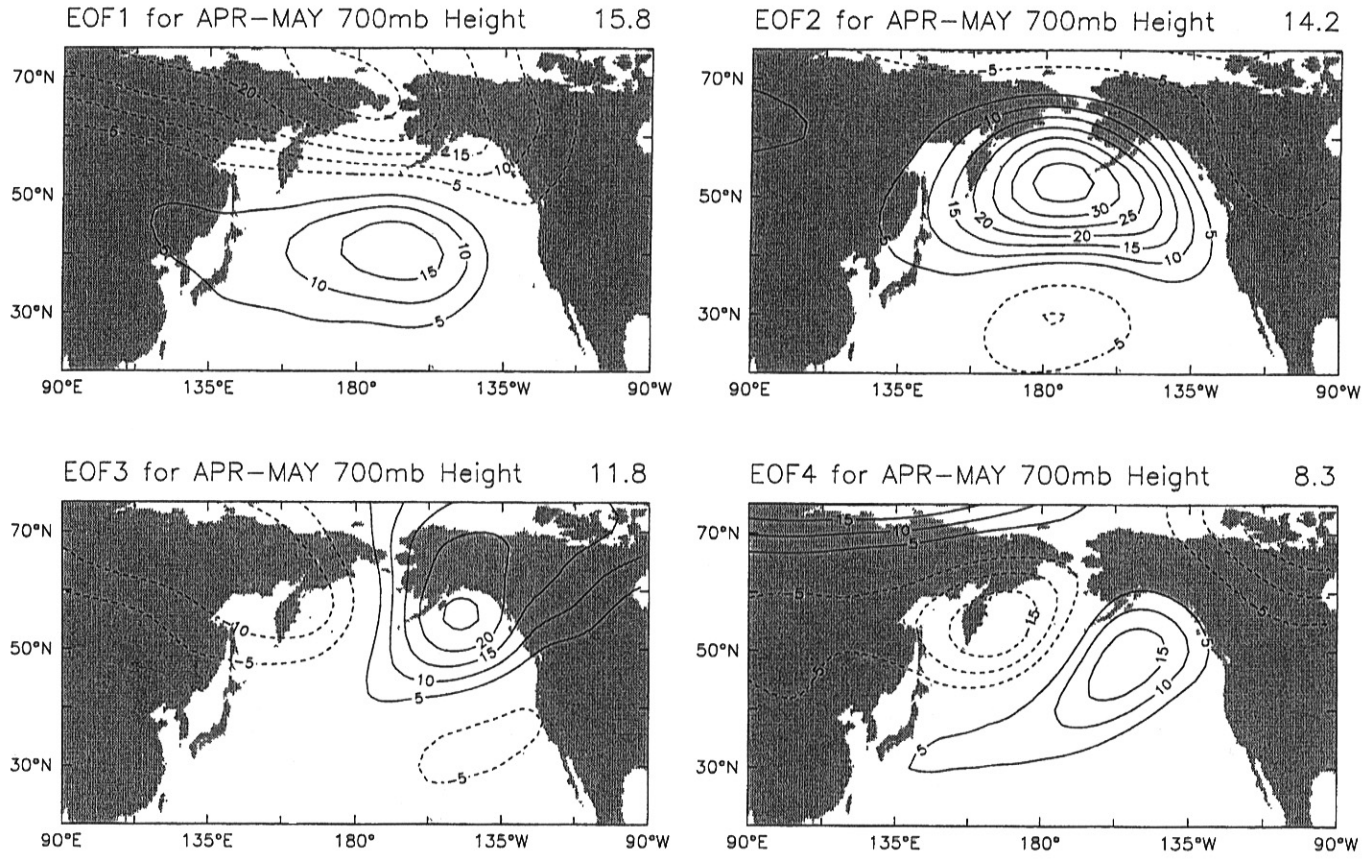
EOF1 for APR–MAY 700mb Height 15.8
EOF2 for APR–MAY 700mb Height 14.2
EOF3 for APR–MAY 700mb Height 11.8
EOF4 for APR–MAY 700mb Height 8.3
70°N
50°N
30°N
90°E
135°E
180°
135°W
90°W

Fig. 2

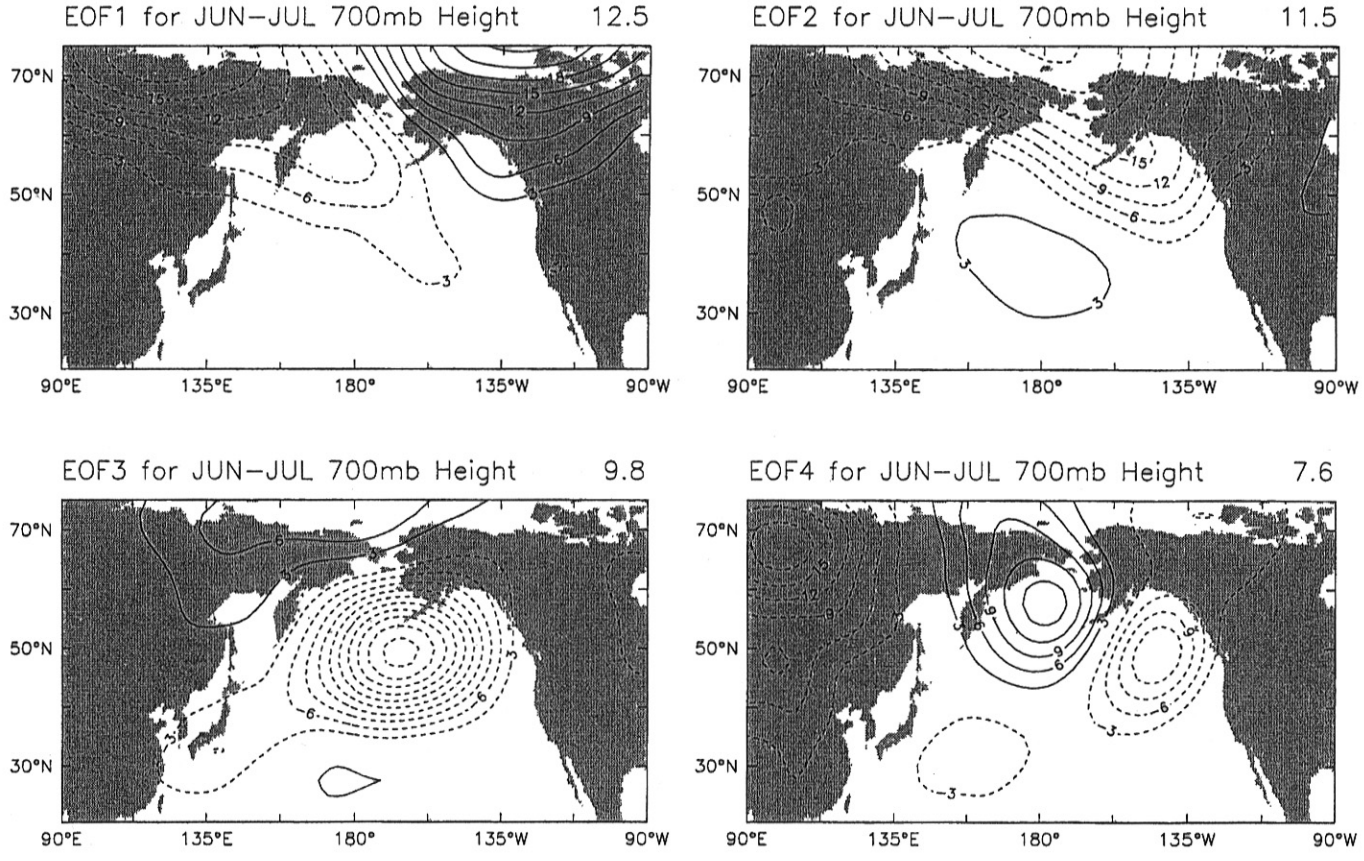
EOF1 for JUN–JUL 700mb Height 12.5
EOF2 for JUN–JUL 700mb Height 11.5
EOF3 for JUN–JUL 700mb Height 9.8
EOF4 for JUN–JUL 700mb Height 7.6
70°N
50°N
30°N
90°E
135°E
180°
135°W
90°W

Fig. 3

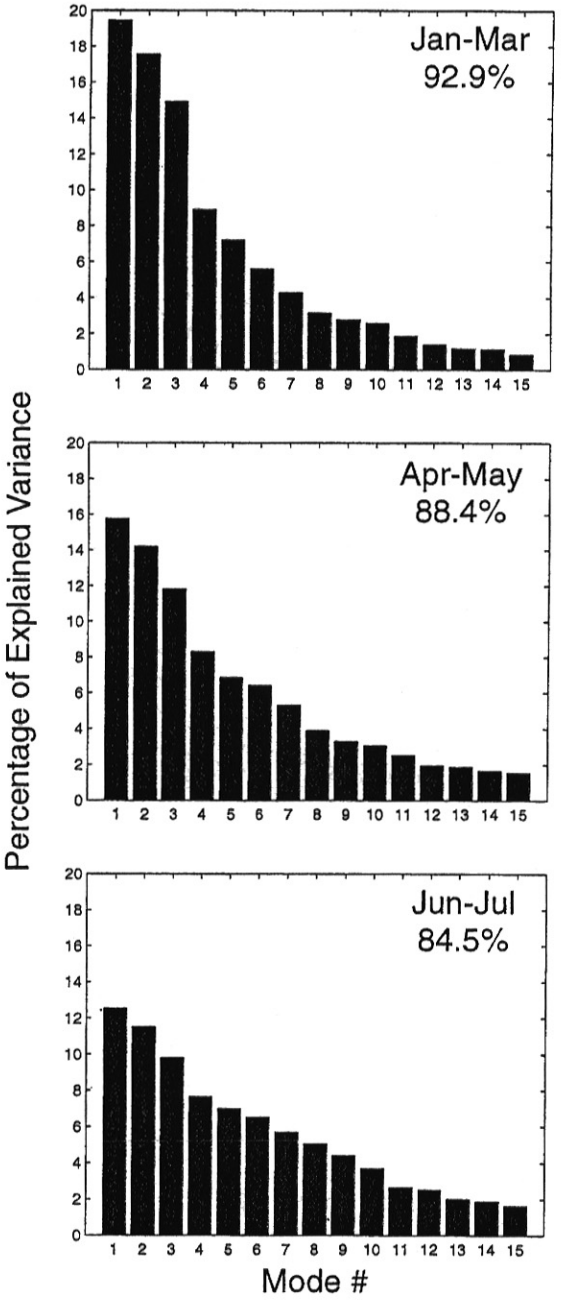
Jan-Mar
92.9%
Apr-May
88.4%
Jun-Jul
84.5%
Percentage of Explained Variance
Mode #

Fig. 4

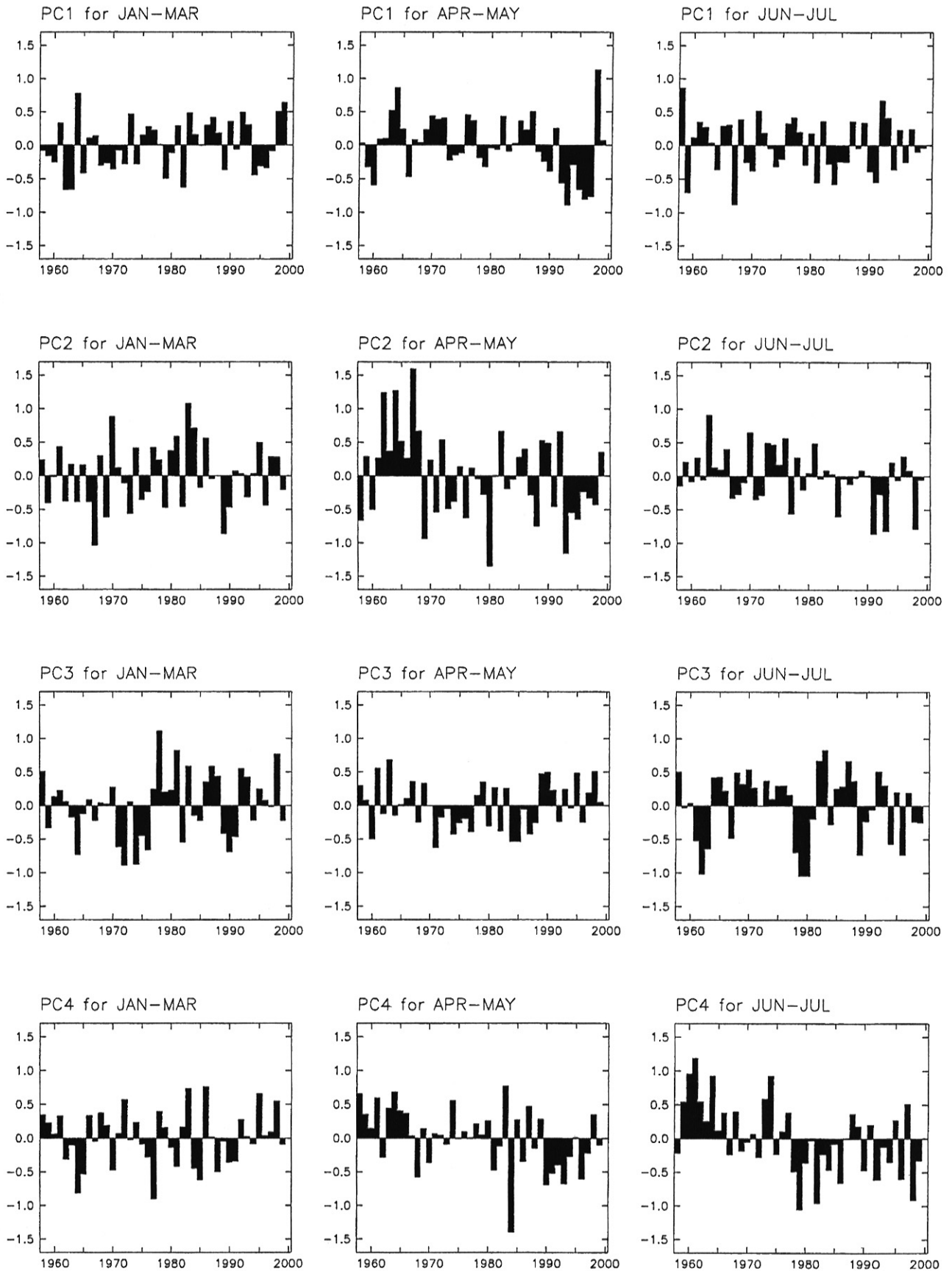
PC1 for JAN–MAR
PC1 for APR–MAY
PC1 for JUN–JUL
PC2 for JAN–MAR
PC2 for APR–MAY
PC2 for JUN–JUL
PC3 for JAN–MAR
PC3 for APR–MAY
PC3 for JUN–JUL
PC4 for JAN–MAR
PC4 for APR–MAY
PC4 for JUN–JUL
1.5
1.0
0.5
0.0
−0.5
−1.0
−1.5
1960
1970
1980
1990
2000

Fig. 5

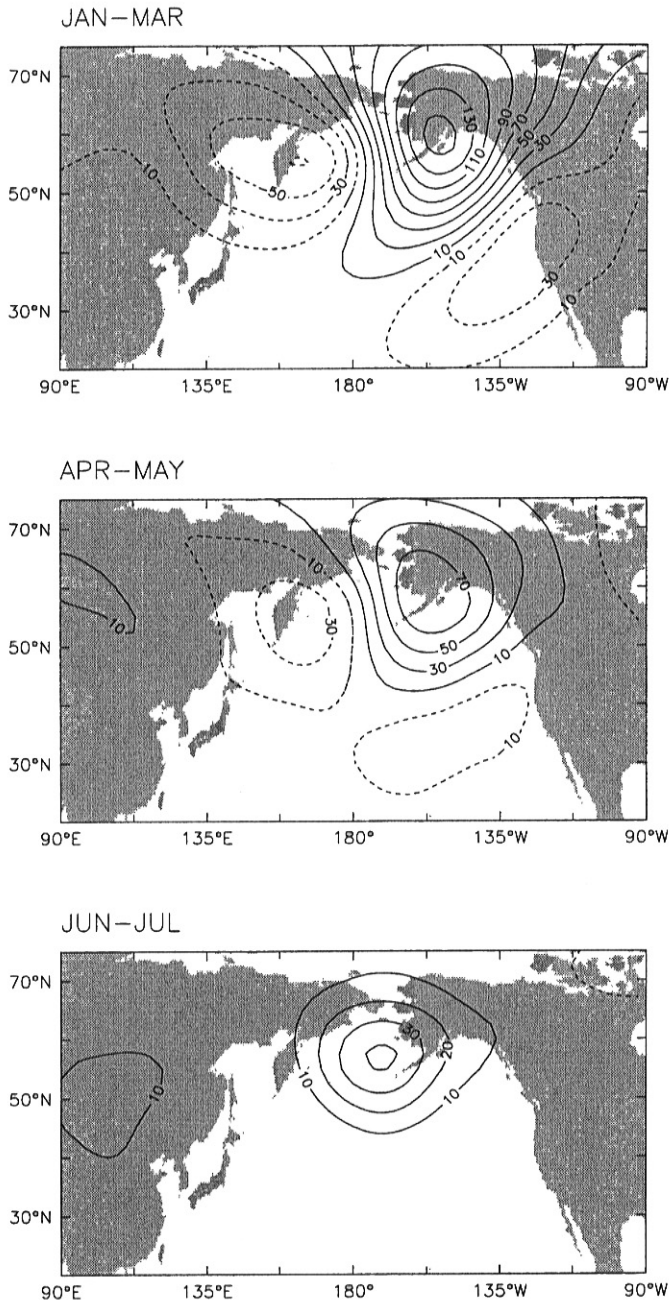

Fig. 6